Interferometric sinograms of transparent objects with stepping wise shifted Ronchi ruling for optical tomography

C. Meneses-Fabian and G. Rodriguez-Zurita
Benemérita Universidad Autónoma de Puebla, Facultad de Ciencias Físico-Matemáticas, Apartado Postal 1152, Puebla, PUE 72000, México

V. Arrizón
Instituto Nacional de Astrofísica, Óptica y Electrónica, Apartado Postal 51 y 216, Tonantzintla, Puebla PUE 72000, México

Recibido el 21 de enero de 2005; aceptado el 28 de septiembre de 2005

An experimental set-up to achieve tomographic images of slices belonging to transparent objects is presented. The proposed system is based on an interferometer which employs two windows in the object plane and a translating absorptive grating (Ronchi ruling) in the frequency plane. In the image plane, replicated windows can be brought to superposition by proper adjustment of the windows' spacing and the grating period. After adaptation of this interferometer to tomographic measurements, the phase of the projections result encoded as interference fringes, thereby forming a composite interference pattern in the plane of the corresponding sinogram (interfero-sinograms). Using phase-stepping techniques, four phase-shifted interfero-sinograms are found after proper translation of the grating. Then wrapped a and unwrapped phase is extracted as a conventional interferogram to obtain a sinogram to be subjected to a filtered backprojection algorithm for reconstruction. As experimental results, the reconstructions of some transparent samples are presented.

Keywords: Image reconstruction; tomography; interferometers; Fourier optics.

Se presenta un arreglo experimental interferométrico para obtener imágenes tomográficas de cortes en objetos transparentes. El sistema propuesto se basa en un interferómetro que emplea dos ventanas en el plano objeto y una rejilla de absorción (rejilla de Ronchi) en el plano de las frecuencias espaciales, capaz de ser trasladada transversalmente. En el plano de la imagen, las ventanas reproducidas en copia pueden superponerse si se elige adecuadamente su espaciamiento respecto al período de la rejilla. Tras adaptar este interferómetro para realizar mediciones tomográficas, la fase de las proyecciones resulta codificada en franjas de interferencia, formando un interferograma en el plano del senograma (interfero-senograma). Usando técnicas de corrimiento de fase aplicadas a interfero-senogramas con corrimientos de fase inducidos por translaciones de la rejilla realizados por etapas, las fases envuelta y desenvuelta pueden ser extraídas para formar un senograma convencional. Este senograma se utiliza para reconstruir la sección mediante un algoritmo estandarizado de retroproyección filtrada. Se muestran algunas reconstrucciones de varias muestras transparentes.

Descriptores: Reconstrucción de imágenes; tomografía; interferometría; óptica de Fourier.

PACS: 42.30.Wb; 07.60.Ly; 42.30.Kq

1. Introduction

A description of the image-formation process of a novel common-path interferometer has been recently presented, using a grating as a spatial filter and two windows at the object plane. In the image plane, superposition of replicated windows and their interference can be achieved by the proper choice of the spacing between windows with respect to the grating period. Furthermore, grating displacement enables the introduction of phase values into diffraction orders as desired, thereby offering the possibility of shifting interference patterns [1]. This device has resemblances with well-known phase-shift methods using grating displacements [2,3], which have been used as phase shifters in phase-shifting interferometers [2]. In fact, a phase-shifting Schlieren technique using a sinusoidal grating has been reported recently [4]. In this type of grating interferometers, a grating is placed as a spatial filter and the phase changes needed for phase-shifting interferometry can be easily performed with the help of an actuator or with a programmable wave modulator such as a liquid crystal display. Because this kind of interferometers seems to have some practical advantages (such as good stability and a relative ease in introducing phase steps), it might be worthwhile to use them in an optical tomographic system for imaging phase distributions. In optical tomography, on the other hand, the phase changes which an optical beam accumulates along its path across a given object has to be measured in order to obtain the phase distribution of a certain object slice by reconstruction techniques [5]. Parallel projection tomography for phase objects in the visible range has been reported using liquid gates to attain low refraction conditions [6]. In this communication, we report experimental tomographic reconstructions of some transparent samples using the implementation of a tomographic system equipped with an interferometer which follows as a variant of the one described in Ref. 1.

2. Overlapping of replicated images with a Ronchi ruling

For a Ronchi ruling of spatial period $d = \lambda f/X_0$, with light bar spatial width given by $A_w = \lambda f a_w$ and displaced by an amount $u_0 = \lambda f \mu_0$ ($1/X_0$, a_w, and μ_0 are conjugate variables of d, A_w and u_0 in an optical Fourier system, respec-

tively) its transmittance can be written in terms of spatial frequencies coordinates as

$$F(\mu,\zeta) = rect\left(\frac{\mu}{a_w}\right) * \sum_{n=-\infty}^{\infty} \delta\left(\mu - \mu_0 - n/X_0\right), \quad (1)$$

where $\mu = u/\lambda f, \zeta = \nu/\lambda f$, with u, v the actual coordinates of the Fourier plane, λ the wavelength of the illuminating optical beam, f the focal length of each Fourier transform lens of the telecentric system, and the symbol $*$ denoting convolution. If the imaging system has the Ronchi ruling as its pupil function, the corresponding impulse response can be written as the following:

$$\tilde{F}(x,y) = \Im^{-1}\{F(\mu,\zeta)\} = a_w \cdot X_0 \text{sinc}(a_w x) \cdot \exp\{i2\pi\mu_0 x\} \sum_{n=-\infty}^{\infty} \delta(x - nX_0, y). \quad (2)$$

This expression reduces to

$$\tilde{F}(x,y) = a_w \cdot X_0 \sum_{n=-\infty}^{\infty} \exp\{i2\pi \cdot n\mu_0 X_0\} \cdot \text{sinc}(na_w X_0) \cdot \delta(x - nX_0, y) \quad (3)$$

for the case of a ruling with equal widths in clear and dark bars, $a_w = 1/(2X_0)$ and there will be no even diffraction orders (missing orders of order 2). Because the ruling used in the experiments had not exactly equal widths in light and dark bars, there are no missing orders. The transmittance of two windows separated from each other by x_0 in the object plane (Fig. 1a) is given by

$$t(x,y) = w(x + \frac{1}{2}x_0, y) + w(x - \frac{1}{2}x_0, y) \cdot \exp\left[i\varphi(x - \frac{1}{2}x_0, y)\right], \quad (4)$$

where $w\,(x,y) = rect\,(x/a)\,rect\,(y/b)$ is the input window system, and $\varphi\,(x,y)$ is the phase term associated with the probe wave window, so that the corresponding amplitude in the image plane can be determined by

$$t_f(x,y) = t(x,y) * \tilde{F}(x,y),$$

which gives

$$t_f(x,y) = a_w X_0 \sum_{n=-\infty}^{\infty} exp\{i2\pi \cdot n\mu_0 X_0\} \cdot \text{sinc}(na_w X_0) \cdot [w(x + \frac{1}{2}x_0 - nX_0, y) + w(x - \frac{1}{2}x_0 - nX_0, y) \cdot \exp\{i\varphi(x - \frac{1}{2}x_0 - nX_0, y)\}] \quad (5)$$

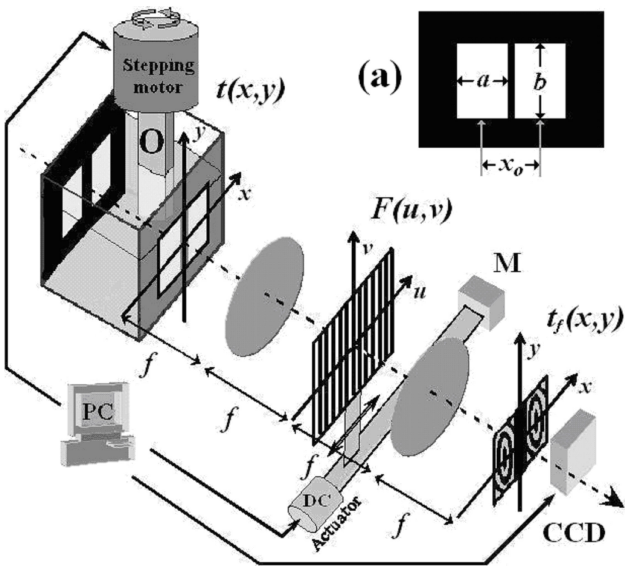

FIGURE 1. Experimental set-up. a) Windows pair.

Thus, in the image plane there are two symmetrically displaced ruling with diffraction orders replicating either one window or the other. The condition for overlapping orders n and $n+N$ is $NX_0 = x_0$, where N is an integer. A useful case of overlapping replicated windows is the case $N = 2$, as shown in Ref. 1 for cosinusoidal absorptive gratings and phase gratings: overlapping occurs for terms with orders $n = +1$ and $n = -1$. Another case of interest is $N = 1$, in which overlapping occurs for the terms with $n = \pm 1$ and $n = 0$. In this case, each term adopts the following form respectively:

$$t_{0f}(x,y) = a_w x_0 \cdot [w(x + \frac{1}{2}x_0, y) + w(x - \frac{1}{2}x_0, y) \cdot \exp\{i\varphi(x - \frac{1}{2}x_0, y)\}], \quad (6)$$

$$t_{+1f}(x,y) = a_w x_0 \exp\{i2\pi \cdot \mu_0 x_0\} \cdot \text{sinc}(a_w x_0) \cdot [w(x - \frac{1}{2}x_0, y) + w(x - \frac{3}{2}x_0, y) \cdot \exp\{i\varphi(x - \frac{3}{2}x_0, y)\}], \quad (7)$$

and

$$t_{-1f}(x,y) = a_w x_0 \exp\{-i2\pi \cdot \mu_0 x_0\} \cdot \text{sinc}(a_w x_0) \cdot [w(x + \frac{3}{2}x_0, y) + w(x + \frac{1}{2}x_0, y) \cdot \exp\{i\varphi(x + \frac{1}{2}x_0, y)\}]. \quad (8)$$

Then, there are overlapping of contributions of replicated windows at each diffraction order. Considering the overlapping of the pair of orders 0,1 or 0,-1 without the further contribution of replicated windows of a higher order, there would be two-beam interference patterns at points $(\pm x_0/2, 0)$.

Within the window region of width $w\,(x - x_0/2, y)$, the irradiance for orders 0 and +1 to be consider can be expressed only as $|t_{0f}\,(x,y) + t_{+1f}\,(x,y)|^2$, and more explicitly, it can be given by

$$I_{01}\,(x,y) = 1 + \text{sinc}^2\,(a_w x_0) + 2\text{sinc}\,(a_w x_0) \times \cos\left[\varphi\,(x,y) + 2\pi\mu_0 x_0\right] \qquad (9)$$

and similarly for 0 and -1. The introduction of a phase step can be performed with the displacement of an amount μ_0. The fringe visibility of these patterns is not unity. It is given by the following function of a_w

$$V_{01}\,(a_w) = \frac{2\cdot\text{sinc}\,(a_w x_0)}{1 + \text{sinc}^2\,(a_w x_0)}, \qquad (10)$$

whose value for the superposition of orders 0 and 1, when

$$a_w = 1/(2x_0),$$

is about 0.91. Under experimental conditions, a fringe contrast good enough for measurements was found.

3. Experimental set-up

Figure 1 shows the experimental set-up, which is basically a telecentric, double Fourier -transform spatial filtering imaging system. The object O under inspection is a transparent rotating object placed just before the $x - y$ object plane. The optical system uses a clean, collimated, linear-polarized He-Ne laser as the light source ($\lambda = 632.8$ nm). Each focal length was $f = 50$ cm. The $x - y$ plane comprises two rectangular windows of sides a and b with a mutual separation of x_o, their respective being positions given by coordinates $(-x_0/2, 0)$ and $(x_0/2, 0)$ respectively (Fig.1a). One of the windows allows the light emerging from the object to pass into the system, while the second window transmits light than has not traveled through the object, thus acting as a reference. The object remains immersed within a liquid gate filled with immersion oil, but it is vertically attached to the axis of a stepping motor in order to rotate from 0 to 360° at 0.9° steps. In the frequency plane of the output plane, a Ronchi ruling with a nominal frequency of 1000 lines per inch (the corresponding spatial period is 25.4 μm) is placed as a spatial filter with its rulings parallel to the vertical line. Given the above parameters, the value of x_0 is about 1.2 cm. A DC actuator can horizontally drive the carrier which supports the Ronchi ruling. A mirror M attached to the carrier is part of one arm of a Michelson interferometer (not shown) for calibration and monitoring of the slide displacements. A PIN detector (Newport CMA series) at the field center of the Michelson interferometer output delivers a signal to an oscilloscope for motion detection and characterization. Typical displacements of the mirror M in fringe numbers as a function of the pulse width applied to the actuator are very linear for several voltages of the pulse within a range from 2 to 120 ms as shown in Fig. 2.

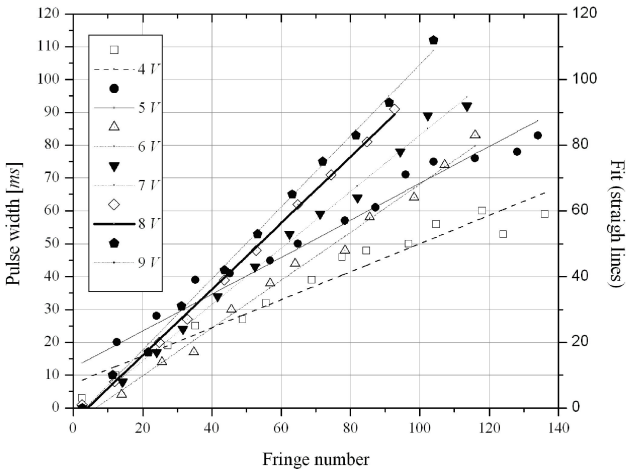

FIGURE 2. Pulse width on the actuator as a function of grating translation in observed fringe shifts at several pulse voltages.

To obtain a phase shift of 180° with a proper pulse width applied on the actuator in order to obtain$\mu_0 = 1/2x_0$, complementary interference patterns were first achieved. According with experimental curves resulting from the Michelson interferometer fringe shifts, a fraction of the pulse width (obtain as described for a 180°C shift) gives a fraction of 180° in the same direction of displacement, there is a lineal depended in the local zone of the operation (Fig. 2). For the experiments presented, pulses of 7.4 V were used with a temporal width of 32 ms for a phase shift of 90° (about 23 fringes counted in the Michelson interferometer, for which the wavelength was 543.5 nm). It was chosen to work with four shifts of values 0, 90, 180 and 270°.

4. Experimental results

The CCD-camera is aligned with one interferogram resulting from overlapping of orders 0 and +1 (Fig. 1). For data acquisition, a line of scanning coordinate $p = x$ is selected from the image received from the CCD-camera at a constant value of, say, $y = h$. This procedure defines an irradiance $I_\phi(p) = I_{01}(p,h)$, taken at a projection angle ϕ, which is stored (a row of 400 data). The object rotates for another irradiance capture. This procedure is repeated at 0.9° steps to cover the range of angles $0°\leq\phi\leq360°$. The values of $I_\phi(p)$ are arranged as rows according to ϕ (an image with a size of 400 × 400 pixels). Experimental interferograms $I_\phi(p)$ construct a composite interferogram (interfero-sinogram) over the plane $p - \phi$, resulting in an interferogram instead of a traditional sinogram [7,8]. To obtain a sinogram, it is assumed that the parallel projection of phase $\widetilde{f}_\phi(p) = \varphi(p,h)$ of the object slice with y=h can be extracted from $I_\phi(p)$ by known techniques, such as phase-shifting interferometry [3]. Experimental results were obtained for a slice of glass microscope slide, which as a sample was used, it was chosen the method of four shifts with 90° steps, such as is explained above section. With this procedure, the four shifts generating the interferograms shown in Fig. 3 (a-d) were obtained. Composite continuous fringes are obtained in spite of the fact

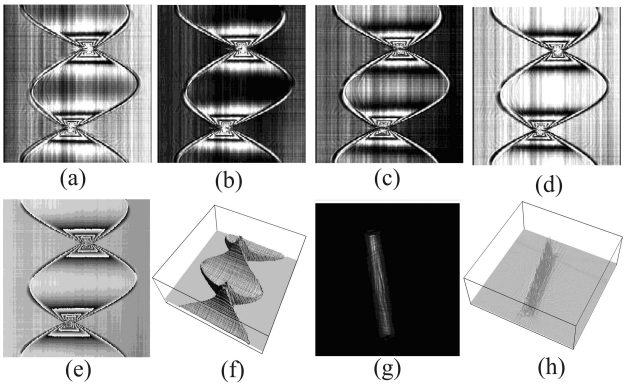

FIGURE 3. (a)-(d) $I_\phi(p) = I_{01}(p, h)$ as functions of p (horizontal axis) and ϕ (vertical axis) as constructed from phase-shifted interferograms. They are referred to as interfero-sinograms. The object is a microscope slice. (e) Wrapped phase, (f) unwrapped phase, on the same p-ϕ plane. (g) and (h) reconstructed object, level gray and three-dimensional plots, respectively.

that each row has been taken separately. Note that the symmetry about $\phi = 180°$ is to be recognized with enough approximation. There are also continuous fringes of low frequency even in the background. Also, the induced phase step shifts the fringes in the sinogram plane as a whole. For each phase-shift, a complete turn of the object had to be made, but the uncertainty in the reproducibility of the zero position of the stepping motor after a complete turn does not appreciably affect the composite interferograms. The interference-fringe frequencies change on a very wide range. In particular, the borders of the object generate the highest frequency fringe values.

In the lower row of Fig. 3, the wrapped phase is first shown as obtained with a standard phase-stepping routine, plot (e). The unwrapped phase in a three-dimensional plot (f), which is to be taken as an estimation of the sinogram $\breve{f}_\phi(p) = \Re\{f(x_h, z_h)\}$, is then subject to a standard filtered backprojection routine [7,8] to give the object slice reconstruction $f(x_h, z_h)$. $\Re$ denotes the Radon transform [7] while $f(x_h, z_h)$ is the unknown phase slice distribution at level h using some coordinates x_h, z_h to describe the slice plane. The corresponding reconstruction is shown in Fig. 3g-h, as a gray tone plot (g) and as a three-dimensional plot (h). This particular reconstruction is calculated with all of the projections within the range [0, 360°]. The dimensions of the object slice are 1 and 8 mm. The geometric proportions of the resulting slice are as expected, and the proportional factor (8 between its sides) can be approximately verifiable.

Further results of using the samples shown in Fig. 4 (glass plate, curved acetate foil, folded acetate foil) are shown in Fig. 5. Acetate foils were cut into small pieces and folded to obtain arbitrary shapes as shown in Fig. 4. Although the general slice form can be identified, there is some loss in borders. This could be due to the high frequencies of the associated fringes, which not only fall outside of the resolution range of the CCD-camera which was used, but also are too high for the phase shifting technique employed.

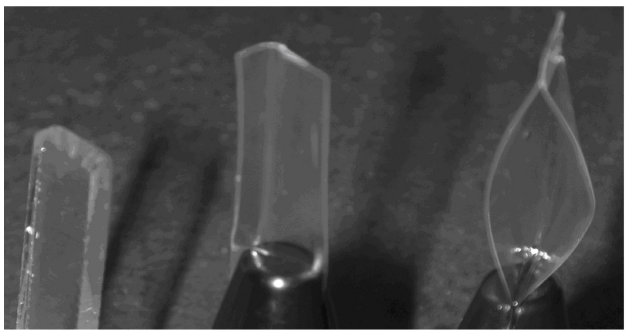

FIGURE 4. Transparent samples for experimental tomographic inspection.

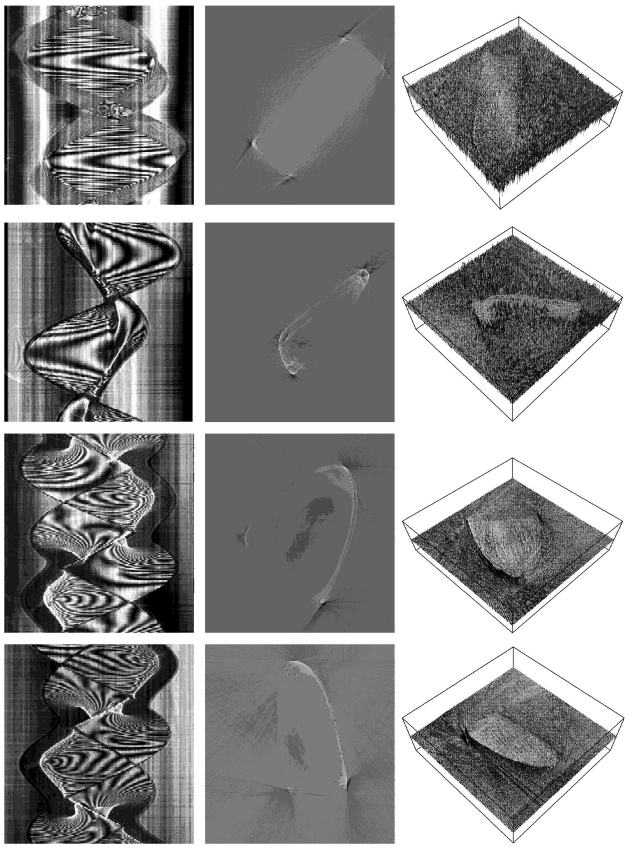

FIGURE 5. Interfero-sinograms (p, horizontal axis and ϕ, vertical axis) at a given phase shift (left column) and reconstructions (middle column: gray tone images, right column: three-dimensional plot) of some sections of the samples of Fig. 4. From above: glass block, foil with "L"-shaped section, and two different sections of the third sample.

5. Final remarks

A common-path interferometer using two windows and a shifting grating was proposed for data acquisition in order to perform tomographic reconstruction of transparent objects in the visible range. In spite of the loss of aperture size and homogeneity in illumination, this system performs with reliability. It shows also good stability.

Acknowledgements

The authors from BUAP wish to thank two graduate students from CINVESTAV-IPN for their valuable help in data acquisition during their summer visit to the facilities where this work was done. This work was partially supported by CONACyT (Grant 41704).

1. V. Arrizón and D. Sánchez-de-la-Llave, *Opt. Lett.* **29** (2004) 141.
2. J. Schwider, R. Burow, K.-E. Elssner, J. Grzanna, and R. Spolaczyk, *Appl. Opt.* **25** (1986) 1117.
3. K. Creath, "Phase-measurement interferometry techniques", in *Progress in Optics XXVI*, E. Wolf, eds. (ELSEVIER Science Publishers, 1998) p. 349.
4. L. Joannes, F. Dubois, and J.-C. Legros, *Appl. Opt.* **42** (2003) 5046.
5. C.M. Vest and P.T. Radulovic, "Measurement of three-dimensional temperature fields by holographic interferometry," in *Applications of Holography and Optical Data Processing*, E. Marcom, A. A. Friesem, and E. Wiener-Avnear, eds. (Pergamon, Oxford 1977), p. 241.
6. C. Meneses-Fabian, G. Rodríguez-Zurita, R. Rodríguez-Vera, and J. F. Vázquez-Castillo, *Opt. Commun.* **228** (2003) 201.
7. S.R. Dean, *The Radon transform and some of its applications* (Wiley, New York, 1983) p.42, 128.
8. A.C. Kak and M. Slaney, *Principles of computarized tomographic imaging* (IEEE Press, New York, 1987).